Brigham Young University

Summer REU 2010

NSF Award #: DMS-0453421

Equitent Problems

Katelynn Kochalski
Dr. Gary Lawlor
Payton Lindsay

December 20, 2010

List of Figures

1 Introduction

Equitent problems ask what is the figure that minimizes perimeter for a given area or volume and a fixed boundary. This paper investigates the equitent problem in $\mathbb{R}^2$, specifically connecting the vertices of regular polygons while also enclosing a given area. We utilize a new method of optimization called metacalibration, which was first developed by Gary Lawlor of Brigham Young University. Equitent problems in the plane can be thought of as a combination of a Steiner problem and an isoperimetric problem, so we will give an introduction to both problems below.

1.1 Introduction to Problem Types

Steiner Problems

The Steiner problem focuses on connecting a given set of points with minimal length. The Steiner problem has several applications, such as the network of roads and telephone wires. Sometimes, the path created to connect the set of points can create additional nodes, called Steiner points. For the minimizing configuration, no more than three segments will meet at any point, and any three segments meeting will always form an angle of 120° with one another. [4] There is an algorithm that gives the minimal Steiner tree solution. However, due to the complexity of large Steiner trees finding the minimal solution is computationally hard. [3]

Isoperimetric Problems

By definition, isoperimetric means having the same perimeter. An isoperimetric problem involves enclosing the most area with a given perimeter. Alternatively, we can solve the dual problem of enclosing a given area with the least perimeter. It is well known that for Euclidean space, the optimal surface is a sphere. In fact, in spaces of constant curvature the solution to the isoperimetric problem often consists of all points at a fixed distance from a center point. Research on the isoperimetric problem continues outside Euclidean space. [2]

Equitent Problems

Equitent is the name given by Lawlor to minimization problems having fixed boundary and enclosing fixed area or volume. They are so named for having both equal ex*tent* and con*tent*.

The planar equitent problem connecting the vertices of three and four sided polygons was solved at the 2008 Brigham Young University REU [1]. In each case, it was proved that a single bubble was preferred to enclose a given area and the position of the bubble was dependent on the amount of area enclosed. In this paper, we extend the previous findings to the equitent problem connecting

the vertices of five- and six-sided polygons.

1.2   Introduction to Methods

Variational Methods

Traditionally, the most common way of solving geometric optimization problems is to use variational methods. For geometric optimization, this method is applied to find a path or curve along which length is minimal. Once the list of regions has been narrowed down to those that are stable and locally minimal, the global minimizer can be isolated using geometric properties. Additionally, due to the indirect process involved in finding the minimum, a proof of the existence of a minimizer is required. [7]

Calibration

The method of calibration compares each region directly to a conjectured minimizer using an intermediate function. We use the intermediate function to create a bridge between the conjectured minimizer and the competitors, showing that every other competitor has longer perimeter than the conjectured minimizer. Thus, we will have shown that our conjectured minimizer is, in fact, the actual minimizer through direct methods. Classical calibration allows for some variables, such as direction and position, and is useful when solving problems with a fixed boundary. Generally it does not, however, allow us to find the minimizer of a region that has enclosed area, volume, or arc-length specifications. [5]

Metacalibration

To solve the equitent problem that connects the vertices of a five- and six-sided polygon, we will use a variation of calibration techniques developed by Lawlor. This method, called metacalibration, uses different vector fields for each competitor. As a result, it introduces new variables to the arguments used in calibration. These new variables allow us to address fixed boundary problems that also have area, volume, or arc-length constraints.

Perhaps due to the difficulty of addressing equitent problems efficiently in three or more dimensions with more traditional methods, these types of problems have been largely neglected, despite their intriguing characteristics.

In reference to any metacalibration problem, we call the proposed optimal surface the *minimizer*, Ω^*, and we refer to every other region possessing the desired properties as a *competitor*, Ω. In a minimization problem, we want to show that $P(\Omega^*) \leq P(\Omega)$ where P represents the perimeter. However, in most cases, proving this directly is difficult. Therefore, we introduce an intermediate function, G, that will allow us to compare our competing perimeters. Each

metacalibration problem makes use of some intermediate function that will allow us to state

$$P(\Omega^*) = G(\Omega^*) \leq G(\Omega) \leq P(\Omega).$$

Proving the middle inequality will always rely on Stokes' Theorem or the Fundamental Theorem of Calculus. Over time, several methods of finding the intermediate function, G, have developed, some proving more useful than others in various situations.

2   Variables

Throughout this paper we frequently refer to a set of variables as we define functions across our figures. Below is a complete list of our definitions of these variables. Note that variables with a hat represent variables on the minimizing figure.

Often we refer to a figure as either representing a regular isotopy class or some alternate isotopy class. An isotopy class is a class of all figures that can be continuously, homeomorphically deformed into each other. Alternatively, we can think of a class of competitors in terms of which pairs of regions share (positive-length) boundary. We will refer to the simplest case, where the number of vertices and the number of regions surrounding the bubble are equal, as the regular isotopy class. An alternate isotopy class can therefore be thought of as any figure where the number of regions surrounding the bubble is less than the number of vertices. Additionally, each alternate isotopy class can be categorized according to which regions are separated by a boundary.

There are two main types of regions in equitent problems: any region outside of the bubble and the bubble itself. The bubble is labeled as B and represents any region which encloses the necessary area. The boundary of this bubble region is called ∂B. Any region outside of the bubble is assigned using the notation R_i. On the regular isotopy class, which we will consider first, this represents a region which is bounded by the vertex lines of the figure, ∂B and the edges of the basis polygon formed by connecting the vertices. On other isotopy classes this definition varies slightly because some regions do not touch the bubble. ∂R_i is the boundary of region R_i. This includes both the polygon edges and ∂B, where applicable.

- S_i is ∂R_i not including the polygon edges
- y is the height of a horizontal slicing line on any competitor
- a is the total area lying below the given slicing line

4

- r is the radius of curvature of the circular arcs of B

- L_i is the length of the intersection of the slicing line y with the region R_i

- L_B is the length of the intersection of the slicing line y with the region B

- H_t is the half plane below a slicing line represented by $H_t = \{y \leq t\}$

- $\hat{y}$ is the height of the horizontal slicing line that cuts off area a on the minimizer

- $\hat{L}_B$ is the length of the intersection of the slicing line $\hat{y}$ with the region B on the minimizer

- $\vec{v_i}$ is a vector field perpendicular to a polygon edge such that the difference between two adjacent vectors $\vec{v_i}$ and $\vec{v_j}$ is unit normal to the boundary between them

- $\vec{\nu}$ is a vector field such that $\vec{\nu} = \vec{v_i} + \vec{n}$ where $\vec{n}$ is the unit normal to ∂R_B

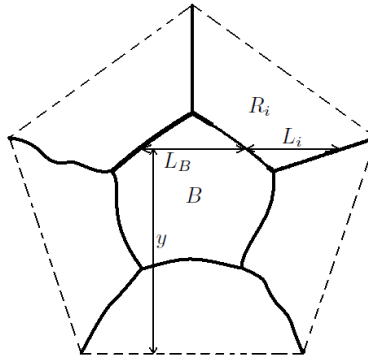Below is a picture to illustrate some of these variables.

Figure 1: Variable Picture

3 Equitent Problem Connecting the Vertices of a Regular Polygon

Our problem requires us to connect the vertices of a regular five- or six-sided polygon while enclosing a given area with minimal perimeter. We first focus on solving our problem for the regular pentagon and will later extend our results to the hexagon. We define the vertices we want to connect by inscribing a regular pentagon on the unit circle. Some possible solutions to this problem are shown below.
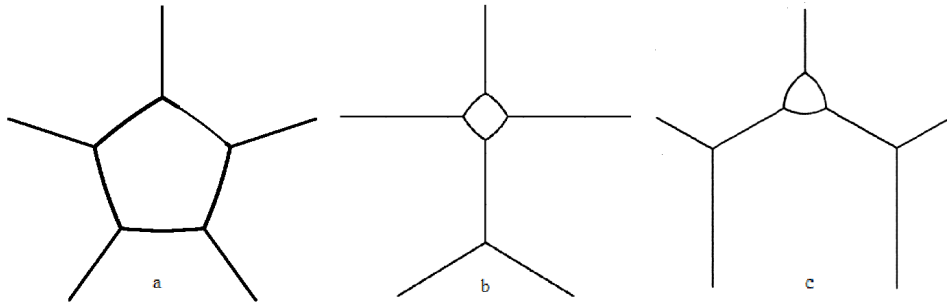
Figure 2: Possible Minimizers

4 Proceeding With the Proof: Building a G Function

Recall that in order to prove $P(\Omega^*) \leq P(\Omega)$ we must use an intermediate function, called the G function, which relates the two perimeters to one another. There are several ways to build an intermediate G function that will allow us to relate the perimeter of the proposed minimizer to the perimeter of any competitor. A G function can be defined using the geometry of the figure or specific vector fields across the figure. Additionally, we can generalize a vector field approach such that finding the G function explicitly from the vector fields is unnecessary. In this proof we focus on a generalized argument for G functions using the flux through each point.

In order to get the inequalities we need vector fields through the figure to have certain characteristics. First, adjacent vector fields must have unit length difference with one another. Second, the difference vector between two adjacent vectors must be perpendicular to the proposed minimizer boundary between them. Upon defining the necessary vector fields we use them to evaluate the flux through the boundary of the minimizer and competitor. The flux through each piece of boundary lying below a horizontal slicing line $y = t$ is the desired intermediate G function for each figure.

5 Proving the Solution

5.1 Generalized G Function Using Flux Arguments

Below we provide a generalized method using flux arguments to define the intermediate G function for the regular isotopy class. This proves that the figure below is minimal among all competitors in which the bubble is surrounded by five separate regions. Due to the abstract method used to define the G function, it also proves the equitent problem connecting the vertices of a n-gon $(n \leq 6)$
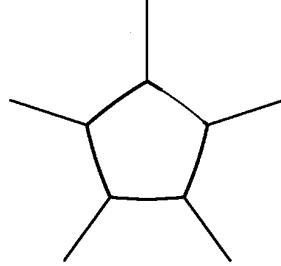
in which the bubble is surrounded by n regions.

Figure 3: Bubble surrounded by five regions

We wish to define a G function based on the flux through a given figure. To do so we must consider two separate components of G. First, we consider the flux through boundaries not containing the bubble.
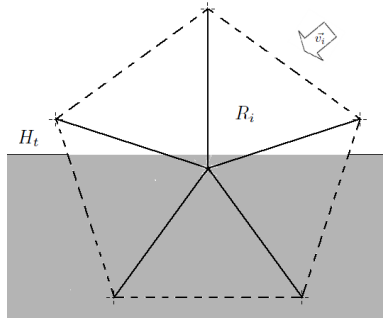

Figure 4: Labeling bubble surrounded by five regions

Definition 1. Let

$$G_s(t) = \sum_i \text{Flux through } S_i \cap H_t \text{ due to vector fields } \vec{v_i}.$$

The second component of our G function focuses on the flux through each point of the bubble.

Definition 2. Let

$$G_B(t) = \sum_i \text{Flux through } \partial B \cap H_t \text{ due to the vector field } \vec{\nu}.$$

We define G to be the sum of both flux components. In other words,

$$G(t) = G_s(t) + G_B(t).$$

For a generic polygon of n edges ($n \leq 6$) it can be geometrically proved that on ∂B

$$\vec{\nu} = \frac{1}{r}\left(-\frac{\hat{L}_B}{2}, \hat{y}\right).$$

Over the whole bubble we define $\vec{\nu} = \frac{1}{r}\left(-\frac{\hat{L}_B}{L_B}(x-c), \hat{y}\right)$ where x is the horizontal distance from the bubble center c.

Consider a narrow horizontal slice of the bubble region B that has been scaled to height 1; horizontally the figure is not drawn to scale.

Figure 5: Bubble region B

On this slice: Flux of $\vec{\nu}$ through $\partial B = \int_B div(\vec{\nu})$

$$\Rightarrow \int_B div(\vec{\nu}) = \int_B \frac{\hat{L}_B}{rL_B} + \frac{\hat{y}'}{r}$$

But $L_B = \hat{L}_B \hat{y}'$, so:

$$\int_B div(\vec{\nu}) = \int_B \frac{1}{r\hat{y}'} + \frac{\hat{y}'}{r}$$

which is the sum of two positive things whose product is constant, so it is minimized when $\frac{1}{r\hat{y}'} = \frac{\hat{y}'}{r} \Rightarrow \hat{y}' = 1$

Thus $div(\vec{\nu}) = \frac{2}{r}$.

$$\frac{2}{r}\Delta a \leq \int_B div(\vec{\nu}) = \text{Flux of } \vec{\nu} \text{ through } B \leq \Delta P + \frac{\Delta \hat{y} L_B}{r}$$

$$\Rightarrow \Delta\left(\frac{2a - \hat{y}L_B}{r}\right) \leq \Delta P$$

Thus to satisfy $G(\Omega) \leq P(\Omega)$ we can also take G_B to be $\frac{2A - \hat{y}L_B}{r}$ and the entire function to be

$$G = \sum_{edges} \text{Flux} + \frac{2A - \hat{y}L_B}{r}.$$

8

5.2 Consistent Vector Behavior

The method of defining vector fields adjacent to a bubble relies on the assumption that the regions and the boundaries separating them are the same for both the ideal and any competitor. If not, the magnitude of $\vec{\nu} - \vec{v_i}$ is not known because $\vec{\nu}$ was defined according to the ideal boundaries. The magnitude of $\vec{\nu} - \vec{v_i}$ can be assumed to be less than unit at a given point only if that point is contained by the circle of the arc from which it was mapped on the ideal. This is because $\vec{v_i}$ can be defined as the distance between the center of the figure and the centers of the vector fields' respective arcs scaled by r.

Theorem 5.1. $\|\vec{\nu} - v_i\| \leq 1 \ \forall \ v_i$.

In order to prove the theorem above we will need the following lemma.

Lemma 1. The distance between the two centers of circular arcs is the radial distance, r.

Recalling that all circular arcs of the interior bubble have the same radius r, it can be geometrically shown that any two adjacent arcs' centers are exactly a distance r apart.
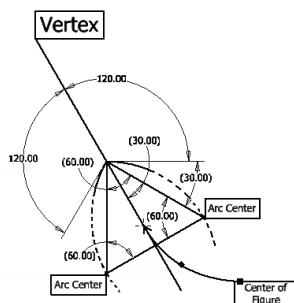

Figure 6: Two adjacent circular arcs' centers are a radial distance apart.

Proof. It is known that the angle between the two circular arcs is 120° and the vertex line a bisector, so the angle between a circular arc and the vertex line is 60°. The radial vector is perpendicular to it's arc, so the angle between it and the vertex is 30°. From symmetry, the angle between two adjacent circular arcs is therefore 60°. It can then be seen that since the two sides of length r are separated by 60°, the distance between the two circle's centers represents the base of an equilateral triangle of length r. $\qquad\square$

We now have the necessary background to prove the theorem we introduced before the lemma. Recall, our theorem states

$$\|\vec{\nu} - v_i\| \leq 1 \ \forall \ v_i.$$

9

Proof. Using the fact that the angle between the vertex line and the circle tangent is 120° and comparing the perpendicular radial line to the circle we find that the angle between the vertex line and the continuation of the circular arc is 60°. Extending the radial line we find that the angle between one circle's radial line and the tangent line of the adjacent circle is 30°. The lemma proved the distance between the two centers of circular arcs is r.

Using this information and symmetry, the geometric figure shown below immediately follows. By taking the outer radial sides of both of the equilateral triangles an arc of 120° on the respective circle is formed. Since the vertex line is 30° beyond the perpendicular radial line of a circle, the angle between two adjacent vertices in this scenario is 180°.
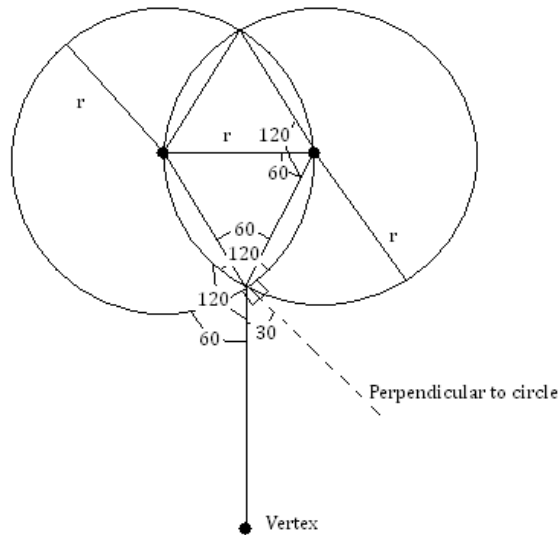

Figure 7: Geometry of two adjacent circular arcs.

For an extended circular arc not to enclose a figure would require two adjacent vertex lines be more than 180° apart. Therefore we can assume that the difference $\vec{\nu} - v_i$ is always less than or equal to unit, thus completing the proof. □

5.3   Flux Proof

Our process for proving a figure is a minimizer involves slicing our figure and its competitors into segments of equal change in G, and then comparing perimeter. Recall the inequality we need to prove is $P(\Omega^*) = G(\Omega^*) \leq G(\Omega) \leq P(\Omega)$.

Theorem 5.2. $P(\Omega^*) = G(\Omega^*) \leq G(\Omega) \leq P(\Omega)$ *where Ω^* refers to the figure below and Ω refers to any figure connecting the vertices of a regular pentagon where the bubble region is surrounded by five regions.*
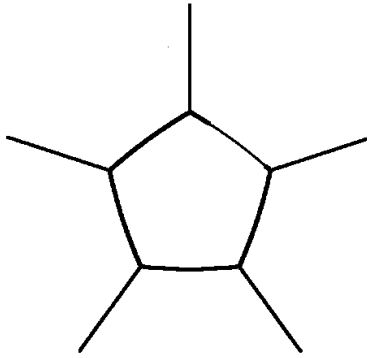

Figure 8: Minimizer where the bubble is surrounded by five regions

Lemma 2. $P(\Omega^*) = G(\Omega^*)$.

We can get several possible slicing types when we slice our figure: where our slicing line does not intersect the bubble region and slices which intersect the bubble region along with various combinations of exterior regions. Because of the way we defined the vector fields however, the proofs for all cases are equivalent.

Proof. In the following proof we will examine a narrow horizontal slice of a figure that has been scaled to height 1; horizontally the figures are not drawn to scale.
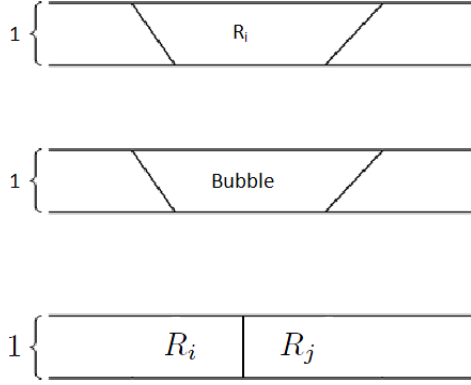
11

1 { R_i

1 { Bubble

1 { R_i | R_j

Figure 9: Possible combinations of regions

It is sufficient for this proof to show that $P'(t) = G'(t)$ because the two functions have the same initial values, so integrating over their boundaries preserves the relationship. Geometrically, $P'(t)$ is the change in perimeter of the boundary segment. Since on the ideal the difference between two adjacent vectors $\vec{v_i}$ and $\vec{v_j}$ is unit normal to the boundary between them and the difference $\vec{\nu} - \vec{v_i}$ is unit normal to the boundary of the interior bubble, the change in flux must be equal to the change in perimeter of the boundaries on the ideal for both ∂B and ∂R_i.

The total change in flux is the sum of the change of flux over all boundaries not containing bubbles with those that do. From above, this will yield a value that is equal to $\delta = \delta_B + \delta_i$ where δ is the total change in perimeter of the boundaries over the segment, δ_B is the change in perimeter of the boundaries containing a bubble and δ_i is the change in perimeter of all boundaries not containing a bubble. Since $P'(t) = \delta$, and since $G'(t)$ can be represented as the change in flux over the segment, $P'(t) = G'(t)$ on Ω^*. Both functions have the same initial values, so we have $P(\Omega^*) = G(\Omega^*)$.

Thus we have considered all possible regions generated by slicing our figure and have found $P(\Omega^*) = G(\Omega^*)$ in each case. $\square$

Lemma 3. $G(\Omega^*) \leq G(\Omega)$.

Proof. Consider the total G across the entire figure, or $G_{top} - G_{bottom}$. Notice, however, that $G_{bottom} = 0$ since there is not flux through the figure at the bottom. Additionally, we know the $\sum_{edges}$ Flux is equivalent for all competitors since the flux through the edges of the basis polygon is constant. Lastly, we

note $L_B = 0$ at the top of the figure. Thus, we have

$$G_{top}(\Omega^*) = \sum_{edges} \text{Flux} + \frac{2A}{r} = G_{top}(\Omega).$$

$\square$

Lemma 4. $G(\Omega) \leq P(\Omega)$.

We can get several possible slicing types when we slice our figure, but again the proofs for all cases are equivalent.

Proof. In the following proof we will examine a narrow horizontal slice of a figure that has been scaled to height 1; horizontally the figures are not drawn to scale.

Again, it is sufficient for this proof to show that $G'(t) \leq P'(t)$. The difference between two adjacent vectors $\vec{v_i}$ and $\vec{v_j}$ is unit normal to the boundary between them on the ideal and the difference $\vec{\nu} - \vec{v_i}$ is unit normal to the boundary of the interior bubble on the ideal. Therefore, since the competitor has boundaries which are oriented differently, the change in flux must be less than the change in perimeter of the boundaries on the competitor for both ∂B and ∂R_i.

The total change in flux is the sum of the change of flux over all boundaries not containing bubbles with those that do. From above, this will yield a value that is equal to $\delta = \delta_B + \delta_i$ where δ is the total change in perimeter of the boundaries over the segment, δ_B is the change in perimeter of the boundaries containing a bubble and δ_i is the change in perimeter of all boundaries not containing a bubble. Since $P'(t) = \delta$, and since $G'(t)$ can be represented as the change in flux over the segment, $G'(t) \leq P'(t)$ on Ω. Both functions have the same initial values, so we have $P(\Omega) \leq G(\Omega)$.

Thus we have considered all possible regions generated by slicing our figure and have found in each case $G(\Omega) \leq P(\Omega)$. $\square$

Proof. (**Theorem 5.2**) Combining the three lemmas above we have our desired inequality which states $P(\Omega^*) = G(\Omega^*) \leq G(\Omega) \leq P(\Omega)$. Therefore, we can conclude that the bubble surrounded by five regions is a minimal solution to the equitent problem we are studying among competitors with the area bubble surrounded by five regions. $\square$

6 Other Minimizers

6.1 Comparing Isotopy Classes

Recall that the equitent problem we are studying requires us to find the minimal distance required to span five fixed points on a polygon while enclosing

a given area. We have already shown that Figure 8 is a minimal solution to our problem when the bubble is surrounded by five separate regions. However, when the bubble is not surrounded by five regions, other figures may be globally minimizing. We will show that there are also two other minimal solutions to this problem. The two additional figures are shown below.
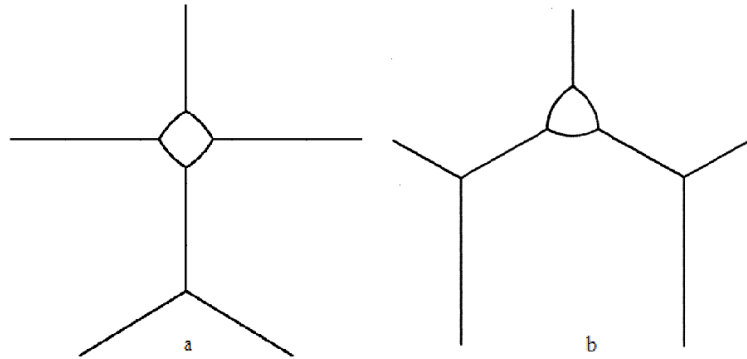

Figure 10: Additional minimizers

We note that these figures both have different isotopy classes.

To find each isotopy class we remove the bubble and place a dot in each region of the figure. Then we connect each pair of dots that share an edge. Upon doing so we notice that each of these three options has a different shape, or isotopy class. Our method requires these to be treated in separate cases. We show the three different isotopy classes below.
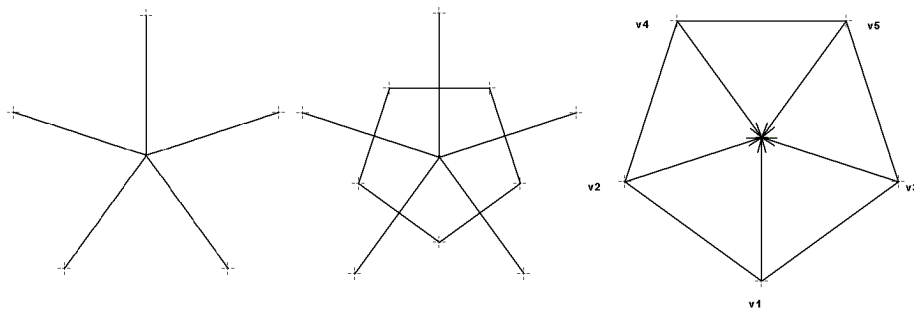
Figure 11: Minimal isotopy class 1
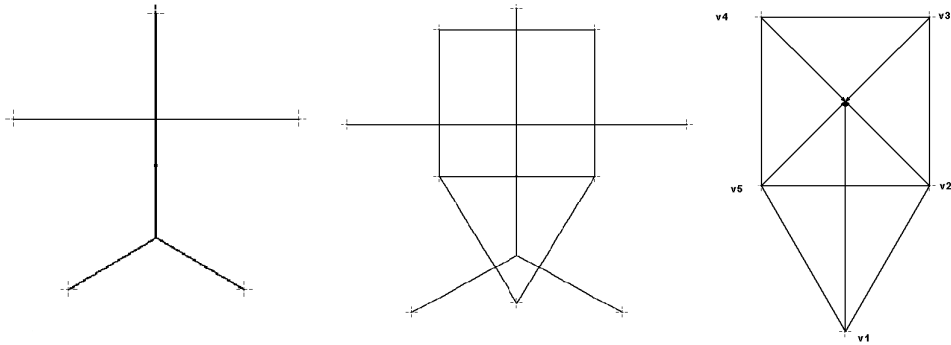
Figure 12: Minimal isotopy class 2
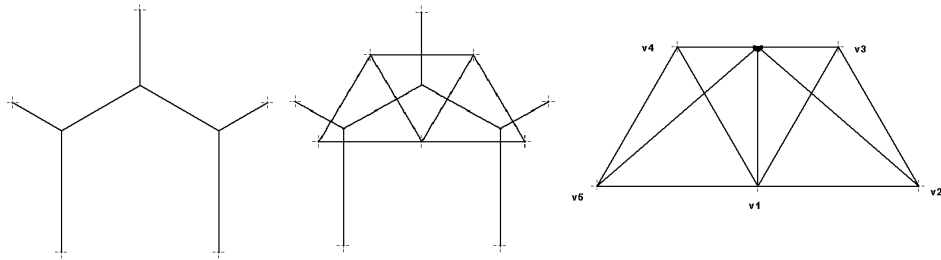
Figure 13: Minimal isotopy class 3

Notice that these are not the only isotopy classes for figures that combine the given area and connect our five fixed points. However, they are the only isotopy classes for the conjectured minimizers. We will provide a proof that our assumption is valid later.

6.2 Vectors Across Boundaries in Alternate Classes

Recall that an alternate isotopy class of a figure with n points will have less than n regions surrounding the bubble. If this is the case then at least one of the lines extending from the bubble will branch and resemble the answer to the three point Steiner problem. In other words, this interior line will intersect with two other lines at an angle of $120°$. Thus, to prove that figures behaving in this way are minimizers we must show there exist three adjacent vector fields who have a unit normal difference with respect to the boundary separating them. Since two of the three vector fields are already defined with respect to the bubble, we need only to prove the existence of the third. Once we know this, we can simply apply the previous proof for regions touching the bubble with this addition for regions

not touching the bubble to our alternate isotopy classes. Together this proves that these isotopy classes are minimizers. The proof can also be generalized to any alternate isotopy class where the bubble is surrounded by 6 or less regions.

Theorem 6.1. *If three line segments meet at an angle of 120°, forming three independent regions, and two known vector fields are fully contained in two separate regions, a third vector field such that the difference between all adjacent vector fields is unit normal to the boundary between them can always be found in the third region.*

Proof. If there is a connection of vertex lines without a bubble, they will invariably meet at a Y with angles of 120°.
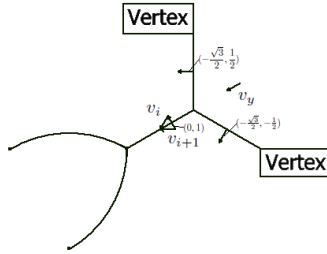
Figure 14: Geometry of a 120° Y connection with vector fields.

To see that the unit normal to the Y is indeed the difference of v_y and v_i, first align the x-axis to the vertex line for simplicity. Then is can be seen that

$$v_i - v_{i+1} = (0,1).$$

The vector v_y can then be defined such that $v_{i+1} - v_y = \left(-\frac{\sqrt{3}}{2}, -\frac{1}{2}\right)$, which is the unit normal to the upper part of the Y.
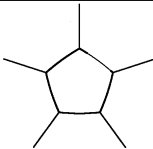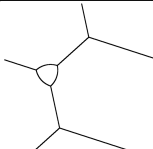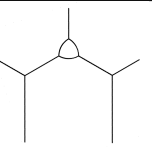Then:

$$v_i - v_y = (v_i - v_{i+1}) + (v_{i+1} - v_y)$$
$$= (0,1) + \left(-\frac{\sqrt{3}}{2}, -\frac{1}{2}\right)$$
$$= \left(-\frac{\sqrt{3}}{2}, \frac{1}{2}\right)$$

which is the unit normal to the lower part of the Y, as desired. □

16

7 Isotopy Class Bounds

We have just proved that there are three minimizers when connecting the vertices of a regular pentagon and enclosing area. Now the question becomes which figure is the global minimizer? The answer to this question depends on the area being enclosed in the figure. The initial assumption that these were the three possible solutions was based on results found using Surface Evolver, a program designed by Ken Brakke. [8] Surface Evolver allows us to view and manipulate a set of fixed points and the area enclosed.

Area Changes		
5 SIDED BUBBLE	4 SIDED BUBBLE	3 SIDED BUBBLE
$0.2334 \leq A \leq 2.498$	$0.0775 \leq A \leq 0.2334$	$A \leq 0.0775$

Here we provide approximations of the exact values of the proposed area bounds. In order to determine where the changes occur we developed formulas for the area and perimeter of the minimizing figures. Using these formulas and the fact that the transformation of the globally minimizing figure between two competing minimizing figures occurs when they have equal area and perimeter, we can determine a value for area. Consider

$$A(n, r_n) = nr_n^2 \left[\frac{\pi}{n} - \frac{\pi}{6} - \frac{\sin\left(\frac{360}{n} - 60\right)}{2} + \frac{\sin^2\left(\frac{180}{n} - 30\right)}{\tan\left(\frac{180}{n}\right)} \right],$$

where n is the number of circular arcs used to enclose the desired area and r_n is the radius of curvature of the arcs. The perimeter formula is dependent on the figure we are considering, these are defined below. We will set $A(3, r_3) = A(4, r_4)$ and $P(3, r_3) = P(4, r_4)$ to determine what area causes the minimal figure to change from one isotopy class to the other. Similarly, we will set $A(4, r_4) = A(5, r_5)$ and $P(4, r_4) = P(5, r_5)$ to find the analogous point when $n = 4$ or $n = 5$.

To determine the perimeter of each figure we first consider its length without the bubble, adding in the length of the circular arcs and subtracting the line segments within the bubble region.

The generic formula that adds the length of the curves and subtracts the line segments within the bubble is

$$\frac{2n\pi r_n}{360} \left(\frac{360}{n} - 60 \right) - \frac{nr_n \sin(\frac{180}{n} - 30)}{\sin(\frac{180}{n})}.$$

17

Combining the above with the perimeter of the figure without the bubble we find:

$$P(3,r_3) = 1 + \cos(36) - \frac{4\sin(18)\tan(42)}{\tan(18)+\tan(42)} - \sin(36)\tan(30) + \frac{2\sin(36)}{\cos(30)} + \frac{8\sin^2(18)}{\cos(42)(\tan(18)+\tan(42))}$$

$$+ \frac{8\sin(18)\tan(42)}{\tan(18)+\tan(42)} + 3r_3\left[\frac{2\pi}{3} - \frac{\pi}{3} - \frac{\sin(30)}{\sin(60)}\right]$$

$$P(4,r_4) = \frac{2\sin(36)}{\cos(30)} + 2\sin(72) + 1 + \cos(36) - \sin(36)\tan(30) + 4r_4\left[\frac{\pi}{2} - \frac{\pi}{3} - \frac{\sin(15)}{sin(45)}\right]$$

$$P(5,r_5) = 5 + 5r_5\left[\frac{2\pi}{5} - \frac{\pi}{3} - \frac{\sin(6)}{\sin(36)}\right]$$

Next, we set $P(3,r_3) = P(4,r_4)$, solving for r_4 in terms of r_3. Then, substituting this value into the formula for $A(4,r_4)$ and setting this equal to $A(3,r_3)$ we obtain a value for r_3. We then use this value in our formula for $A(3,r_3)$ to obtain $A \approx .0775$. Thus, we know when $A \leq .0775$ the figure with three regions surrounding the bubble region is minimal.

We repeat this process, using $P(4,r_4)$, $P(5,r_5)$, $A(4,r_4)$, and $A(5,r_5)$ to find $A \approx .2234$. From this we can conclude when $.0775 \leq A \leq .2234$ the figure with four interior lines extending from the bubble region is minimal. Whenever $.2234 \leq A \leq 2.498$ the minimal solution will be the figure with five lines extending from the bubble region.

A visual representation of these changes can be seen by graphing each area and perimeter equation. In this graph intersections represent points where the minimal figure changes.
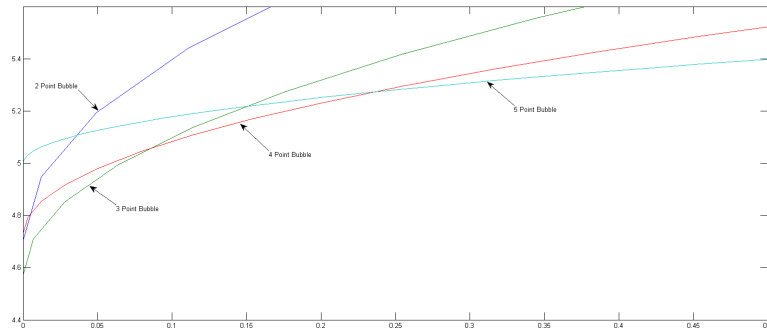

Figure 15: Perimeter (y-axis) vs. Area (x-axis)

7.1   Isotopy Classes

Throughout the paper we have only considered three isotopy classes as globally minimal. The globally minimal solution, as shown above, will depend on the amount of area being enclosed.

Theorem 7.1. *The isotopy classes we considered are the only cases that have the potential to be globally minimal.*

Proof. To complete this proof we must consider several alternate ways to connect the five points and enclose area. This includes figures where line segments meet at angles other than 120°, the figure contains multiple bubbles and the bubble does not intersect the figure at all, the bubble is not placed at a vertex.

Case 1 Line segments within the figure meet at angles other than 120°
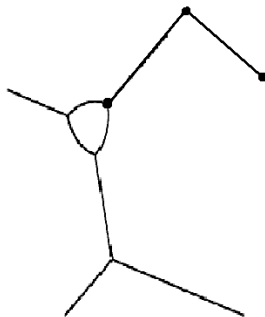
Figure 16: Line segments do not meet at 120°

Notice if we concentrate on connecting the three dotted points, the minimal solution should resemble the solution to the three point Steiner tree problem. This would mean it is most efficient to create an addition node where the three line segments meet at 120°.

Figure 17: Optimal intersections vs. non-minimizing intersections

The picture above depicts the optimal way to connect the three desired

19

points. This minimal solution is an application of the three point Steiner problem.

Case 2 The figure contains multiple bubbles

Consider a figure that connects the five required points while enclosing the necessary area in more than one bubble. Here we again employ the flux argument, setting

$$G = \sum_{edges} \text{Flux} + \frac{2A - \hat{y}L_B}{r}.$$

When we add an additional bubble, the above G function becomes

$$G_2 = \sum_{edges} \text{Flux} + \frac{2A_1 - \hat{y}_1 L_{B_1}}{r_1} + \frac{2A_2 - \hat{y}_2 L_{B_2}}{r_2}.$$

We can compare G_2 to the initial G function at the end of the figure to see which is most efficient. Notice that Total $G = G_{top} - G_{bottom}$, $G_{bottom} = 0$, and at the top of the figure $L_B = 0$. Thus we have

$$G_2 = \sum_{edges} \text{Flux} + \frac{2A_1}{r_1} + \frac{2A_2}{r_2} > \sum_{edges} \text{Flux} + \frac{2(A_1 + A_2)}{r} = \sum_{edges} \text{Flux} + \frac{2A}{r} = G$$

whenever $r > r_1, r_2$. $A_1 + A_2 = A$, so $A > A_1, A_2$ and a larger area will, by definition, have a larger radius. Thus, we conclude $r > r_1, r_2$ for any two bubbles. Notice that this argument can easily be expanded for more than two bubbles to show it is always more efficient to have a single bubble containing the required area.

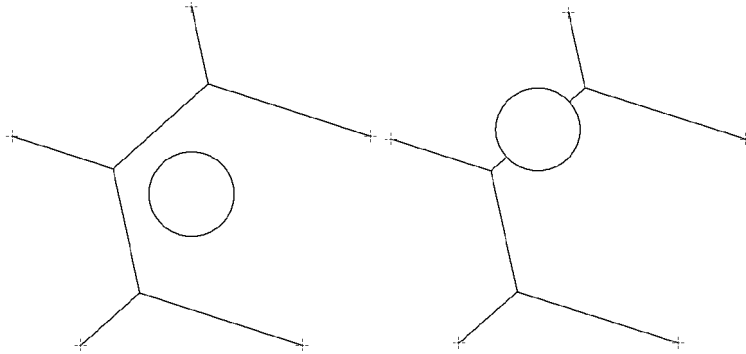**Case 3** The bubble does not intersect the boundary line of the figure

Figure 18: Bubble region outside and intersecting the boundary line

For the case where a bubble is outside the figure it is trivial to prove that the bubble simply centered at any boundary line will save $2r$ length while enclosing the same amount of area. Since there exists some figure that is better the proposed figure must not be the minimizer.

Case 4 The bubble is not centered at a vertex

Notice in the picture above the bubble merely intersects a line segment. In order to better analyze this case, we merely treat the section of the graph containing the bubble as an equitent problem connecting the vertices of a triangle while enclosing a given area. This problem was studied and solved in 2008 by students at the Brigham Young University REU. It was shown that the minimal solution to this problem was to enclose the area at a vertex. [6] Therefore, a figure where the bubble is not centered at a vertex is not a minimizer.

Thus we have examined all isotopy classes that enclose a given area and span our specified fixed points and found the only global minimizers to be the three minimizers we considered.

□

8 Connecting the Vertices of a Regular Hexagon While Enclosing a Given Area

Here we show the conjectured solutions to the equitent problem which connects the vertices of a regular hexagon while enclosing a given area. For this problem we have not considered relatively small areas. Again, we made the initial conjectures using Surface Evolver. The globally minimal solution is dependent on the area enclosed by the figure. The conjectured minimizers for this problem when not enclosing a small area are shown below.
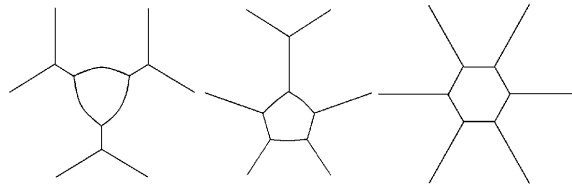

Figure 19: Minimizers when connecting the vertices of a regular hexagon
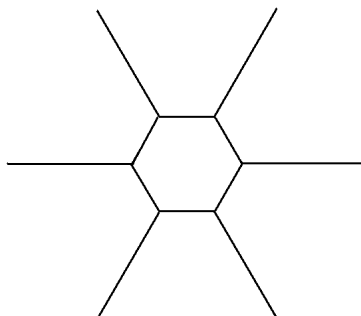
8.1 Regular Isotopy Class

Figure 20: Minimizer of the regular isotopy class

Here we will give some explanation of why the generalized proof provided for the regular isotopy class in the previous problem works. Consider the figure which has six regions surrounding the bubble and the general G function defined in section 5.1. Notice in this figure for line segments to meet at $120°$ angles the area is enclosed with straight lines. By definition, a straight line has radius ∞. Thus our G function simply becomes

$$G = \sum_{edges} \text{Flux.}$$

A simple argument shows that $\|v_i\| = 1$. Therefore, evaluating the flux through any boundary point on the minimizer simply gives the perimeter. Due to the nature of the proof for the regular isotopy class, we can use the same argument to obtain the desired inequality for this problem. Thus, we have shown this figure is a minimizer within its isotopy class.
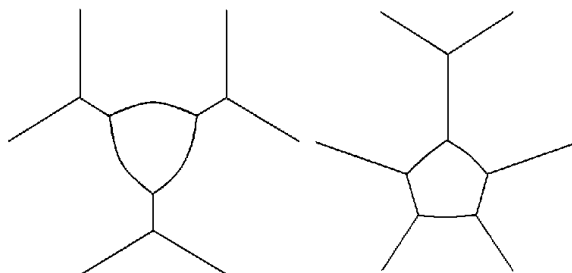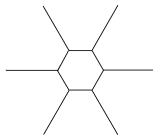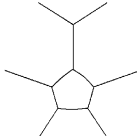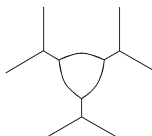
8.2 Alternate Isotopy Classes

Figure 21: Minimizer of the alternate isotopy classes

Notice that two of the alternate isotopy classes fit the stipulations of the alternate isotopy classes defined earlier. Therefore we can conclude that these two figures are minimizing within their isotopy classes by the same arguments used with the previous problem.

8.3 Isotopy Class Bounds

The same methods used to find area bounds for the equitent problem connecting the vertices of a pentagon while enclosing area were used to determine which figure is globally minimal based on the area enclosed for the hexagon problem. We provide approximations of the exact values of the bounds for each figure below.

Area Changes		
6 SIDED BUBBLE	5 SIDED BUBBLE	3 SIDED BUBBLE
$0.259 \leq A \leq 2.598$	$0.215 \leq A \leq .259$	$A \leq .215$

It is interesting to note that a figure with a four-sided bubble is not among our global minimizers. While this figure is locally minimal, upon doing the above analysis we found that there is always a figure that has less perimeter.

8.4 Additional Case

We conjecture that there is an additional case which is globally minimal for small areas. However, we did not have time to fully consider this case. We

believe this figure resembles the solution to the six point Steiner problem with the area enclosed at the vertex.
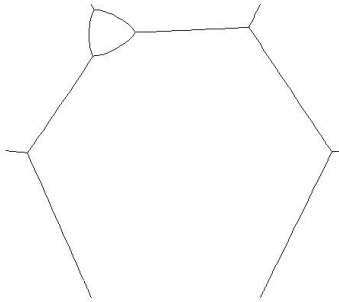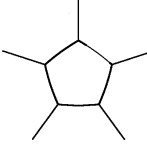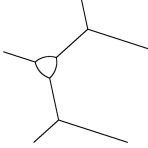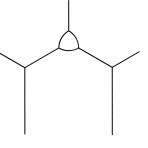

Figure 22: Conjectured global minimizer for small areas

9   Conclusion

In conclusion, we have found the most efficient way to connect the vertices of a regular pentagon while enclosing a given area. We present the table of our findings below.

Area Changes		
5 SIDED BUBBLE	4 SIDED BUBBLE	3 SIDED BUBBLE
$0.2334 \leq A \leq 2.498$	$0.0775 \leq A \leq 0.2334$	$A \leq 0.0775$

Notice that in each figure the area is enclosed by circular arcs. This reflects the solution to the isoperimetric problem which states that a circle encloses a given area with minimal perimeter. Additionally, in each figure all line segments meet at 120° angles. This coincides with the solution to the Steiner tree problem where all line segments meet at 120° angles to minimize the path connecting a fixed set of points.

We were also able to identify several local minimizers for the problem that connects the vertices of a regular hexagon while enclosing a given area. We believe that these will also be global minimizers depending on the amount of area being enclosed.

It is interesting to note that the general construction of our proofs can be applied to alternate isotopy classes of any equitent problem where the bubble

24

is surrounded by six or less regions.

Future work in this area could determine the nature of the globally minimizing solution to the regular hexagon problem. Additionally, it would be interesting to study equient problems on other manifolds, such as the hyperbolic plane.

10   Acknowledgements

References

[1] BYU REU 2008. Three and four point equient problems.

[2] Viktor Blasjo. The evolution of the isoperimetric problem. *Amer. Math. Monthly*, 112:526–566, 2005.

[3] Jeff Erickson. Np-hard problems. available at http://compgeom.cs.uiuc.edu/ jeffe/teaching/algorithms/.

[4] M. Hazewinkel. *Encyclopaedia of Mathematics*. Springer, New York, NY, 2001.

[5] Gary Lawlor. Metacalibrations: A unifying framework for minimization proof. Available at http://mathed.byu.edu/ lawlor/PaperShorter.pdf.

[6] Jr. Reese Harvey, H. Blaine Lawson. Calibrated geometries. *Acta Mathematica*, 148:47–157, 1982.

[7] Eric W. Weisstein. Calculus of variations. Mathworld, available at http://mathworld.wolfram.com/CalculusofVariations.html.